PERGAMON

Energy Conversion & Management 40 (1999) 1057–1072

ENERGY CONVERSION & MANAGEMENT

Engine exhaust system design based on heat transfer computation

I.P. Kandylas, A.M. Stamatelos*

Laboratory of Applied Thermodynamics, Mechanical Engineering Department, Aristotle University of Thessaloniki, Thessaloniki, Greece

Received 27 March 1998; accepted 10 December 1998

Abstract

The heat transfer conditions in automotive exhaust piping are only recently being studied in depth because of their important role in the design and optimization phases of exhaust after-treatment systems. The complex geometry of the exhaust line and the special flow conditions complicate the problem of accurately estimating several important heat transfer parameters. This paper initially summarizes the current status of knowledge regarding heat transfer phenomena in automotive exhaust systems. Experimental data from steady state and transient heat transfer measurements in automotive exhaust systems are presented and analyzed by means of a comprehensive transient computer model covering all exhaust piping configurations (single wall, double wall with air gap or insulation) already presented elsewhere. Examples are presented, illustrating the application of the model in the comparative assessment of different exhaust configurations. In conjunction with existing models which simulate the operation of three-way catalytic converters and of other exhaust gas after-treatment devices, the model is already integrated in a CAE package for the support of exhaust system design optimization.

Keywords: Heat transfer; Automotive exhaust systems; Mathematical modeling

1. Introduction

Although the first works on this subject are more than 10 years old [1,2], the study of heat transfer in automotive exhaust systems has only recently attracted the importance it deserves

* Corresponding author. Tel.: +30-31-996-066; Fax: +30-31-996-019.
E-mail address: tassos@antiopi.meng.auth.gr (A.M. Stamatelos)

0196-8904/99/$ - see front matter
PII: S0196-8904(99)00008-4

Nomenclature

Variables

A	heat transfer surface
CAF	convective augmentation factor
c_p	specific heat capacity
d	diameter
f	pipe friction factor
g	gravitational acceleration
h	convective heat transfer coefficient
l	length
$\dot{m}$	mass transfer rate
NEDC	New European Driving Cycle
Nu	Nusselt number
Pr	Prandtl number
$\dot{q}$	heat transfer rate
r	radius
Ra	Rayleigh number
Re	Reynolds number
s	thickness
t	time
T	temperature
u	exhaust gas velocity
V	volume
x	axial distance from entrance

Greek letters

α	thermal diffusivity
ε	emissivity factor (radiation)
β	thermal expansion coefficient
λ	heat conduction coefficient
Λ	λ_{ins}/λ_p
ρ	density
σ	Stefan–Boltzmann constant
ν	kinematic viscosity

Subscripts

amb	ambient
cv	convection
eff	effective
g	exhaust gas
gap	air gap between pipes
i	inner, pipe inlet

ins	insulation
o	outer, pipe outlet
p	pipe
p,i	inner pipe
p,o	outer pipe
rad	radiation
sur	surroundings

due to its key role in the design of modern exhaust after-treatment systems [3]. Such studies are today important for better understanding of these systems and, thus, being able to influence underbody heat transfer, transient cold-start warm-up of the catalytic converter, thermal ageing of the converter, or the regeneration behaviour of diesel particulate traps etc [4].

Oncoming automotive exhaust emissions standards focus on the minimization of cold start emissions for catalyst-equipped gasoline cars. In that context, all passive means of achieving faster catalyst warming must be first exhaustively examined due to their lower cost in

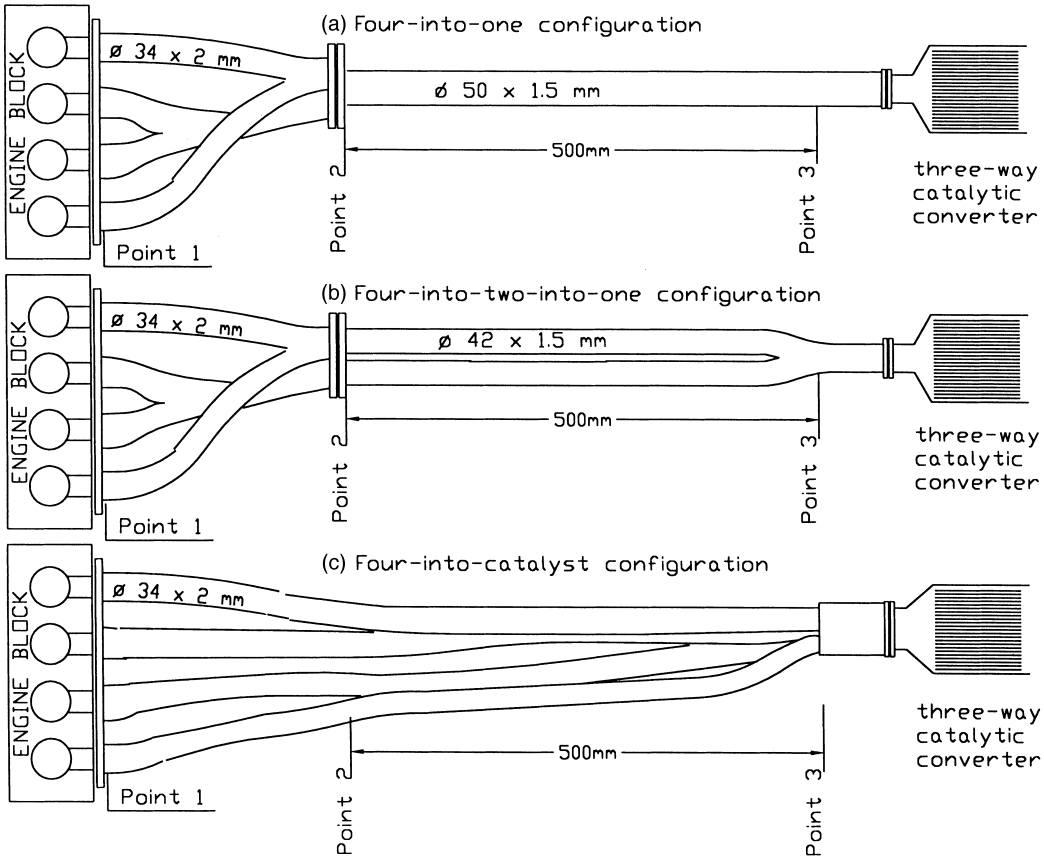

Fig. 1. (a–c). Gasoline car exhaust system configurations (four-into-one, four-into-two, four-into-catalyst).

comparison to active configurations. A significant number of exhaust manifold, takedown piping and converter packaging design variations have emerged during the last years with varying performance and secondary effects. For the example of a four-cylinder engined car, Fig. 1(a–c) presents three possible exhaust system configurations (four-into-one, four-into-two-into-one, four-into-catalyst configuration).

This fact led to an increasing interest in studying and estimating heat transfer within exhaust systems. The resulting heat transfer rate expressions are embodied in computational models that contribute to the overall system tuning, the reduction of the product design and optimization phases and to facilitate the selection of systems with high probability of success in the market [5].

Another important application area is related to the design of particulate trap systems for Diesel powered vehicles. Here again, the design of the exhaust manifold and piping significantly affects the exhaust gas inlet temperature into the trap and, consequently, the temperature levels attainable inside the ceramic filter. Last, but not least, during the design of exhaust manifolds for turbocharged engines, the thermal inertia of the exhaust system upstream of the turbine must be taken into account in order to ensure optimized turbocharger matching and turbo lag minimization.

Experimental investigation of the heat transfer rates in exhaust ports was initially aimed at supporting thermodynamic engine cycle models, especially for engine turbocharger matching applications [6]. Those experimental findings were exploited in the computer model developed by Frank [7], who also simulated manifold heat transfer by employing classical correlations applicable to curved pipes. Meisner and Sorenson [8], on the other hand, based on the experimental results of Sachdev [9], presented a comprehensive model covering also heat transfer in takedown pipes. Both models focused, however, mainly on the temperature variation during single engine operating cycles. Pattas et al. studied the thermal response behavior of diesel exhaust systems equipped with a particulate filter [4]. Zhang et al. developed a model computing the steady state temperature distribution in exhaust systems with single wall and with double wall, air gap insulated piping [10]. Recently, one-dimensional transient models covering a variety of exhaust system designs have been presented [3,11,12], presenting a model that was able to simulate real world heat transfer in exhaust systems of gasoline cars and is extensively employed in CAE investigations [3].

The experimental acquisition of useful data for the estimation of heat transfer rates and their application in the optimized design of various exhaust configurations forms the subject of the present paper.

2. Estimation of heat transfer rates

In this section, we are going to review the relations and parameters which are involved in the computational modeling of the above described modes of heat transfer in exhaust piping. The relations and laws presented here are essential to the formulation of the sets of differential equations which mathematically describe the behavior of the different versions of exhaust piping design.

2.1. Component-interior heat transfer

The typical flow conditions in automotive exhaust systems produce Re numbers in the range of 10^3–5×10^4. The exhaust flow often enters the region $Re < 2300$, especially in the exhaust manifold runners. In spite of that, the flow remains actually turbulent, since it has flowed through a substantial restriction. The exhaust valves and the persisting, unsteady, flow pulsation effects do not favour the transition to the laminar region.

The heat transfer in the exhaust port is highly unsteady. When the exhaust valve opens, a high velocity jet sets up recirculation zones in the port that result in enhanced heat transfer rates. When the exhaust valve is fully open, the flow resembles a turbulent, pipe flow. As the exhaust valve closes, there is another period when a narrow jet of gases sets up recirculation zones, thereby again affecting the heat transfer process. During the period when the valve is closed, the flow rate approximates zero and correspondingly low heat transfer occurs. In order to quantify the above phenomena, four different correlations for the heat transfer coefficients applicable to each of the above mentioned periods have been proposed [13]. The proposed heat transfer models based on this work [6] predicted about half the measured values. In a later work, Caton examined problems of weighted time averaging by use of a number of thermocouples measuring port and manifold temperatures [14].

For the other parts of the exhaust system downstream the exhaust port, pipe flow correlations are usually applied based on the average flow rate of the exhaust gas during the engine operating cycle. Among the numerous heat transfer coefficient correlations for the fully developed flow in a straight channel, we mention the Sieder–Tate relation which correlates the Nu number with Re and Pr [15]:

$$\mathrm{Nu} = 0.027\ \mathrm{Re}^{0.8}\mathrm{Pr}^{1/3} \tag{1}$$

The correlation proposed by Gnielinski [16] takes additionally into account the effect of wall roughness by means of the friction factor f.

$$\mathrm{Nu} = \frac{\frac{f}{8}(\mathrm{Re} - 1000)\mathrm{Pr}}{1.07 + 12.7\sqrt{\frac{f}{8}}(\mathrm{Pr}^{2/3} - 1)} \quad \text{for } 10^4 < \mathrm{Re} < 5 \times 10^6 \tag{2}$$

and

$$\mathrm{Nu} = \frac{\frac{f}{8}\mathrm{Re}\ \mathrm{Pr}}{1.07 + 12.7\sqrt{\frac{f}{8}}(\mathrm{Pr}^{2/3} - 1)} \quad \text{for } \mathrm{Re} < 10^4 \tag{3}$$

As the flow enters the pipe, the thin thermal boundary layer gives higher local Nu numbers, and it takes an order of 15 to 30 diameters for the Nu to approach the asymptotic value of the fully developed flow [17].

For low Re numbers, Reynolds et al. correlated their analytical results as [18]:

$$\frac{\mathrm{Nu}(x)}{\mathrm{Nu}_\infty} = 1 + 0.8\left(1 + 7 \cdot 10^4 \mathrm{Re}^{-3/2}\right)\left(\frac{x}{d_1}\right)^{-1} \tag{4}$$

Another relation for the heat transfer enhancement in the entrance region is proposed in Ref. [19]:

$$\frac{\mathrm{Nu}(x)}{\mathrm{Nu}_\infty} = 0.892 + 2.02\left(\frac{x}{d_1}\right)^{-1} \tag{5}$$

The turbulent boundary layer also decreases in thickness in the vicinity of a bend. This tends to enhance the heat transfer between the pipe wall and the exhaust gas. The following relation to account for pipe bend effects is recommended in Ref. [20]:

$$\frac{\mathrm{Nu}_{\text{bent-pipe}}}{\mathrm{Nu}_{\text{straight-pipe}}} = 1 + \frac{21 \cdot d_1}{\mathrm{Re}^{0.14} d_{\text{bend}}} \tag{6}$$

However, the heat transfer coefficient is also affected for some length downstream of the bend, which decreases with increasing Re [21].

The highly unsteady, pulsating nature of the flow in the exhaust manifold has been suggested as an explanation for the increased heat transfer rates observed in exhaust systems. Condie and McEligot conducted an experimental study with real exhaust systems but with steady, non-pulsating flow. Their results imply that the enhanced heat transfer rates are also observed in the absence of pulsations [22].

The heat transfer coefficients measured in the takedown section of real exhaust systems by Sachdev [9] were correlated by Meisner and Sorenson [8] to yield the following relation:

$$\mathrm{Nu} = 0.0774\ \mathrm{Re}^{0.769} \tag{7}$$

The above expression gives significantly higher values than those predicted for straight pipes with fully developed flow. Sandford and Jones [23] modified the Reynolds analogy proposed by Benson [24] and, thus, computed instantaneous heat rejection in manifold runners and the takedown pipe.

Because of the complexity of the geometry and flow conditions, recent studies [11,25] suggest the use of the common relations for straight pipes in an application-oriented with the introduction of suitable Convective Augmentation Factors, as defined below:

$$\mathrm{CAF} = \frac{\mathrm{Nu}_{\text{effective}}}{\mathrm{Nu}_{\text{theoretical}}} \tag{8}$$

It has been found that these factors are different for the exhaust manifold, the takedown pipe and the tailpipe and only very slightly depend on Re for values up to 10^4 [25]. This approach is consistent with the results of the measurements conducted by a number of researchers in real automotive systems that suggest an exponent for the Re very close to 0.8 for the Nusselt correlation [3].

In order to clarify the situation regarding which is the proper correlation to use in transient exhaust system modeling, data from steady state measurements in real exhaust systems components have been compiled in this paper, along with the existing, above mentioned

correlations. It was observed that Sachdev's data compare well with Wendland's measurements and the data of the authors and could be accurately described by the Meisner correlation in the range $10^3 < \mathrm{Re} < 10^4$.

2.2. Convection and radiation to surroundings

In the usual case of a vehicle moving at variable velocity, forced convection to the underhood airflow and radiation must be taken into account. The heat transfer coefficient is then derived from the respective Nusselt number which is computed on the basis of the following relations [26]:

$$\mathrm{Nu} = 0.3 + \sqrt{\mathrm{Nu}_{\mathrm{laminar}}^2 + \mathrm{Nu}_{\mathrm{turbulent}}^2}, \text{ for } 10 < \mathrm{Re} < 10^7 \tag{9}$$

where

$$\mathrm{Nu}_{\mathrm{laminar}} = 0.664\sqrt{\mathrm{Re}}\sqrt[3]{\mathrm{Pr}} \tag{10}$$

$$\mathrm{Nu}_{\mathrm{turbulent}} = \frac{0.037\ \mathrm{Re}^{0.8}\mathrm{Pr}}{1 + 2443\ \mathrm{Re}^{-0.1}(\mathrm{Pr}^{2/3} - 1)} \tag{11}$$

The Reynolds number is defined using the wetted length of the exhaust pipe. In the case of cross-flow, the wetted length equals the semi-perimeter of the pipe.

The radiation heat transfer rate in an elemental control volume of length Δx is given by the following equation:

$$\dot{q}_{\mathrm{rad}} = \varepsilon\sigma\pi d_2\left(T_{\mathrm{p}}^4 - T_{\mathrm{amb}}^4\right)\Delta x \tag{12}$$

Skin emissivity may vary significantly depending on the type of material and its condition (e.g., degree of oxidization, roughness), as well as skin absolute temperature. Emissivity values of several materials as a function of temperature are contained in Table 1 [25,27,28].

3. Experimental assessment of heat transfer coefficients

The results from a series of steady state measurements conducted on two cars (a 2 liter and a 1.1 liter engined car) on the road with different velocities are presented in Fig. 2(a–d).

Table 1
Emissivity values of different pipe materials

Material	Emissivity
Cast iron aged at 600°C	$0.5 + (T_{\mathrm{p}} - 273)/2860$
Mild steel lightly aged	$0.17 + (T_{\mathrm{p}} - 273)/6950$
18-8 stainless, unpolished	0.22
18-8 stainless, oxidized	0.86
AISI 304 St. Steel heated to 500°C	$0.54 + (T_{\mathrm{p}} - 273)/2830$

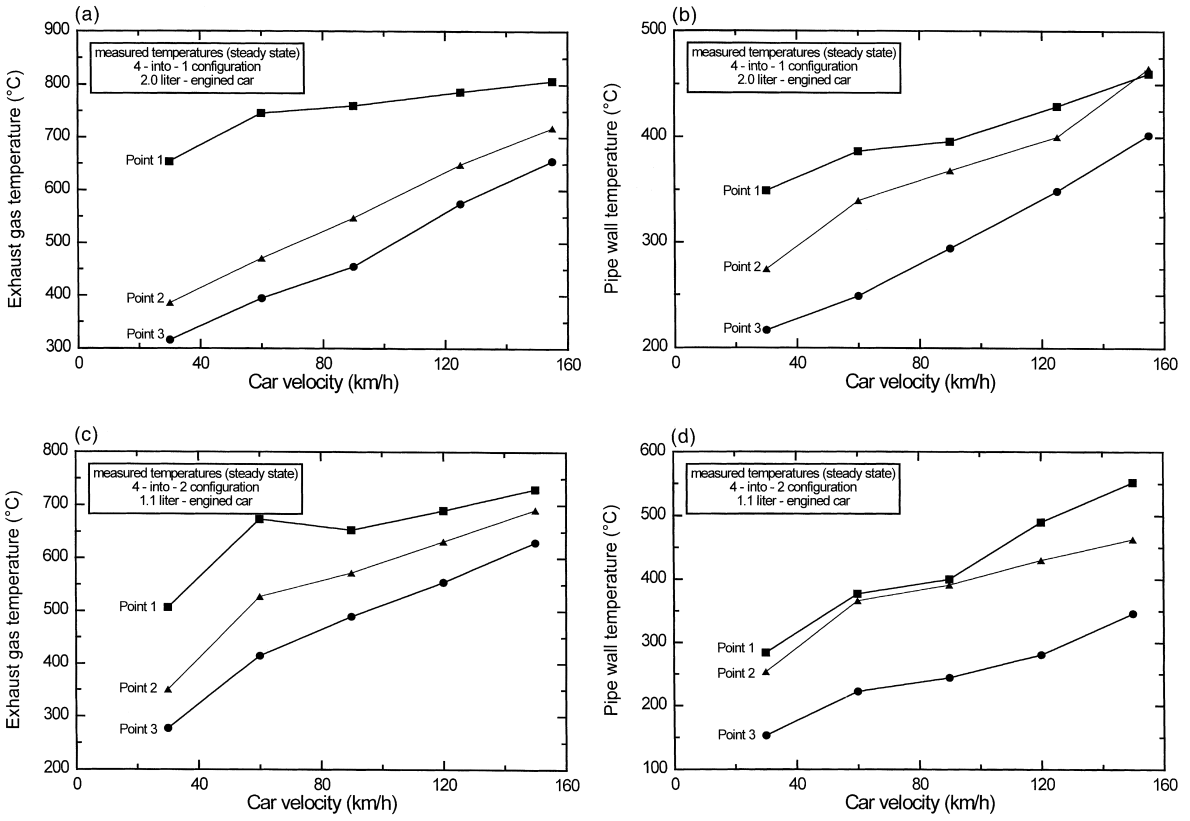

Fig. 2. (a–d). Steady state measurements results (exhaust gas and pipe wall temperatures as function of car velocity—(a, b) 2.0 liter engined car; (c, d) 1.1 liter engined car).

Exhaust gas and pipe wall temperatures at three points along the exhaust system of the two cars have been measured for the following steady-state operation points: constant speed driving at 30, 60, 90, 120 and 150 km/h. Temperatures were measured at the exhaust manifold inlet and exit, as well as the downpipe exit.

Fig. 2(a) presents the exhaust gas temperatures at the three measurement points, for the 2-liter engined car with a four-into-one exhaust system configuration. Fig. 2(b) presents the pipe wall temperatures for the same car at the respective points and car velocities. Exhaust gas mass flow rates have also been recorded for the calculations of heat transfer rates. The geometry of the exhaust line between the measurement points follows the general layout of Fig.1(a), with different dimensions as follows. It comprises $\varnothing 39 \times 36$ mm exhaust manifold runners of 0.5 m mean length, followed by a single pipe $\varnothing 53 \times 50$ mm downpipe of 0.6 m length.

Fig. 2(c) presents the exhaust gas temperatures at the three measurement points, for the 1.1-liter engined car with a four-into-two exhaust system configuration. Fig. 2(d) presents the pipe wall temperatures for the same car at the respective points and car velocities. Exhaust gas mass flow rates have also been recorded. The geometry of the exhaust line between the measurement points follows the general layout of Fig.1(a), with different dimensions as follows. It comprises

$\varnothing 36 \times 30$ mm exhaust manifold runners of 0.3 m mean length, followed by a double pipe $\varnothing 47 \times 44$ mm downpipe of 0.38 m length.

The following methodology, which is analogous to the one presented in [25] was employed to deduce the pipe interior and exterior heat transfer rates in the manifold and the downpipe sections.

Based on the measured exhaust gas and pipe wall temperatures and the component inlet and exit (1–2)for manifold, 2–3 for downpipe, an energy balance for the exhaust gas is employed for the calculation of the mean heat flux:

$$\dot{q} = \dot{m} c_{\mathrm{p}} \left(T_{g_1} - T_{g_2} \right) \tag{13}$$

The resulting heat fluxes are employed in the estimation of a mean gas to wall convection coefficient, based on the log mean temperature difference [29]:

$$\dot{q}_{\mathrm{cv}} = \bar{h} A_{\mathrm{i}} \Delta T_{\mathrm{lm}} \tag{14}$$

$$\Delta T_{\mathrm{lm}} = \frac{\Delta T_{\mathrm{o}} - \Delta T_{\mathrm{i}}}{\ln(\Delta T_{\mathrm{o}} / \Delta T_{\mathrm{i}})} \tag{15}$$

In this expression, the gas-wall temperature differences at pipe section outlet ΔT_{o} and inlet ΔT_{i} are calculated based on the mean pipe wall temperature. This simplification is considered as reasonable, in view of the accuracy requirements of this procedure, and based on the fact that the estimation of heat transfer rates is not very sensitive in the values of pipe wall temperatures.

The resulting data are presented in Fig. 3 as Nu–Re correlations. They compare very well with literature data [3].

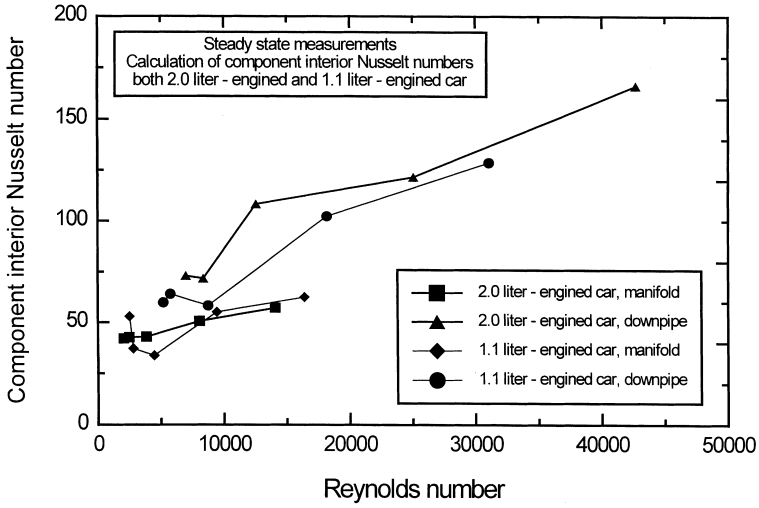

Fig. 3. Correlation of the calculated component-interior Nusselt number with the Reynolds number, based on the steady-state measurements with the two cars.

The same heat flux curves are employed in the calculation of the external heat transfer rates, which occur via forced convection to the ambient underbody air-flow and radiation to the surroundings. In the specific experiments, the contribution of radiation may be neglected, due to the relatively low pipe wall temperatures (less than 500°C) and the shielding of the exhaust manifold.

$$\dot{q} = h_{\mathrm{amb}}\pi d\left(T_{\mathrm{p}} - T_{\infty}\right)l + \varepsilon\pi \mathrm{d}\sigma\left(T_{\mathrm{p}}^4 - T_{\mathrm{sur}}^4\right)l \tag{16}$$

The resulting data are presented in Fig. 4 in the form of convection coefficient versus vehicle velocity. Apparently, the general trend predicted by Eq. (9) is followed. This type of data is employed in the correction of the results of this equation to account for the complex underhood geometry, view factor and flow conditions.

4. Analysis of the results of transient tests

The exhaust gas flow in the exhaust system is unsteady and compressible. The flow condition at each location is described by three independent parameters, namely velocity, density and pressure. These three variables are governed by the equations of mass, momentum and energy. In automotive exhaust systems, the variation of pressure lies in the order of a few milibars and is, thus, of negligible importance in the computation of the other variables. For the narrow pressure ranges of the exhaust gas, the density can be determined as a function of temperature. Assuming quasi-steady, incompressible flow, the energy balance equation for the exhaust gas can be written as:

$$\frac{\partial T}{\partial t} + u\frac{\partial T_{\mathrm{g}}}{\partial x} = -\frac{\dot{q}_{\mathrm{cv,i}}}{\rho_{\mathrm{g}} c_{\mathrm{p_g}} V_{\mathrm{l}}} \tag{17}$$

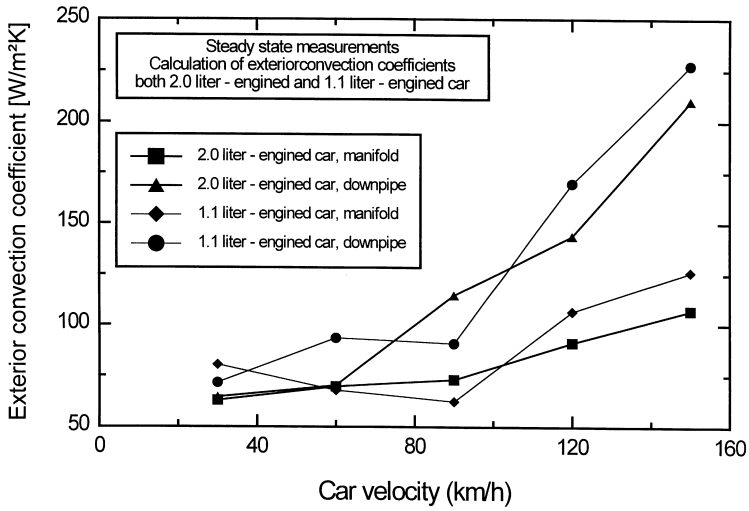

Fig. 4. Correlation of the calculated component-exterior Nusselt number with the car velocity, based on the steady-state measurements with the two cars.

Table 2
Exhaust pipe transient heat transfer model [5]

Equation type	Case	Equation	Heat transfer mode	Rate expression
Energy balance (exhaust gas)	All cases	$\frac{\partial T_g}{\partial t} + u\frac{\partial T_g}{\partial x} = -\frac{\dot{q}_{cv,i}}{\rho_g c_{p_g} V_1}$	Convection exhaust gas-to-pipe wall	$\mathrm{Nu} = \frac{\frac{f}{8}(\mathrm{Re}-1000)\mathrm{Pr}}{1.07+12.7\sqrt{\frac{f}{8}}(\mathrm{Pr}^{2/3}-1)}$ (CAF)
			Convective augmentation factor	
Energy balance (pipe wall)	Single wall	$\frac{\partial T_p}{\partial t} = \alpha_p\frac{\partial^2 T_p}{\partial x^2} + \frac{\dot{q}_{cv,i} - \dot{q}_{cv,o} - \dot{q}_{rad}}{\rho_p c_p (V_2 - V_1)}$	Radiation to surroundings	$\dot{q}_{rad} = \varepsilon\sigma\pi d_2\left(T_p^4 - T_{amb}^4\right)\Delta x$
	Double wall-air gap	(*) $\frac{\partial T_{p,i}}{\partial t} = \alpha_{p,i}\frac{\partial^2 T_{p,i}}{\partial x^2} + \frac{\dot{q}_{cv,i} - \dot{q}_{cv,gap} - \dot{q}_{rad,i}}{\rho_{p,i} c_{p,i}(V_2 - V_1)}$	Forced convection from pipe wall to ambient air ($10 < \mathrm{Re} < 10^7$)	$\mathrm{Nu} = 0.3 + \sqrt{\mathrm{Nu}_{laminar}^2 + \mathrm{Nu}_{turbulent}^2}$
	(*) inner pipe (**) outer pipe	(**) $\frac{\partial T_{p,o}}{\partial t} = \alpha_{p,o}\frac{\partial^2 T_{p,o}}{\partial x^2} + \frac{\dot{q}_{cv,gap} + \dot{q}_{rad,i} - \dot{q}_{cv,o} - \dot{q}_{rad,o}}{\rho_{p,o} c_{p_{p,o}}(V_4 - V_3)}$		$\mathrm{Nu}_{laminar} = 0.664\sqrt{\mathrm{Re}}\sqrt[3]{\mathrm{Pr}}$
				$\mathrm{Nu}_{turbulent} = \frac{0.037\,\mathrm{Re}^{0.8}\mathrm{Pr}}{1+2443\,\mathrm{Re}^{-0.1}(\mathrm{Pr}^{2/3}-1)}$
	Double wall-insulation	(*) $\frac{\partial T_{p,i}}{\partial t} = \alpha_{p,i}\frac{\partial^2 T_{p,i}}{\partial x^2} + \frac{\dot{q}_{cv,i} - \dot{q}_{p,i\to ins}}{\rho_{p,i} c_{p,i}(V_2 - V_1)}$	Natural convection (air gap)	$\mathrm{Nu}_{gap} = 0.2\,\mathrm{Ra}^{0.25}\left(\frac{d_3}{d_2}\right)^{0.5}$
	(*) inner pipe (**) insulation (***) outer pipe	(**) $\frac{\partial T_{ins}}{\partial t} = \alpha_{ins}\frac{\partial^2 T_{ins}}{\partial x^2} + \frac{\dot{q}_{p,i\to ins} - \dot{q}_{ins\to p,o}}{\rho_{p,i} c_{p,i}(V_3 - V_2)}$		$\mathrm{Ra}_{gap} = \frac{s_{gap}^3 g\beta_{gap}(T_{p,i} - T_{p,o})}{\alpha_{gap}\nu_{gap}}$
		(***) $\frac{\partial T_{p,o}}{\partial t} = \alpha_{p,o}\frac{\partial^2 T_{p,o}}{\partial x^2} + \frac{\dot{q}_{ins\to p,o} - \dot{q}_{cv,o} - \dot{q}_{rad,o}}{\rho_{p,o} c_{p_{p,o}}(V_4 - V_3)}$		$s_{gap} = \sqrt{r_2 r_3}\,\ln\left(\frac{r_3}{r_2}\right)$
				$h_{gap} = \frac{\mathrm{Nu}_{gap}\lambda_{gap}}{s_{gap}}$

The radial temperature gradients in the pipe wall are neglected due to the low thickness and high thermal diffusivity of the metal. Taking into account the convective heat transfer between the exhaust gas and pipe wall, as well as the heat losses to the ambient by convection and radiation, the energy balance for the wall of a single-walled pipe or manifold runner is written as:

$$\frac{\partial T_p}{\partial t} = \alpha_p \frac{\partial^2 T_p}{\partial x^2} + \frac{\dot{q}_{cv,i} - \dot{q}_{cv,o} - \dot{q}_{rad}}{\rho_p c_p (V_2 - V_1)} \tag{18}$$

A comprehensive transient exhaust system heat transfer model solving these equations with the kinetic expressions of Table 2, is already presented elsewhere [3]. In order to assess the validity of this model, a set of transient experiments were conducted with a 1.8 liter engined car on the chassis dyno. The driving cycle that corresponds to the NEDC exhaust emission test was employed in this case. Exhaust temperatures at various points along the exhaust system were recorded on a second-by-second basis. The same is true for the mass flow rates.

Two different exhaust manifold and downpipe configurations have been tested, namely, a four-into-one configuration (Fig. 1a), and a four-into-two configuration (Fig. 1b).

Fig. 5 shows indicative results of the measurements with the four-into-one exhaust system configuration. Measured exhaust gas temperatures at points 1 and 2 are shown as a function of time in the New European Driving Cycle. For comparison, calculated results for the temperature at point 2 based on the measured results at point 1 are also shown. A very good agreement of the computed and measured temperatures at point 2 is observed.

In order to assess the effect of a different exhaust system design, the same experiment was conducted with the same car equipped with a four-into-two-into-one exhaust system (Fig. 1b). Indicative results for points 1 and 2 are shown in Fig. 6. The respective model computation results with reference to this exhaust system configuration are also shown in this figure. Again, the comparison shows a good agreement between computation and experiment both for the

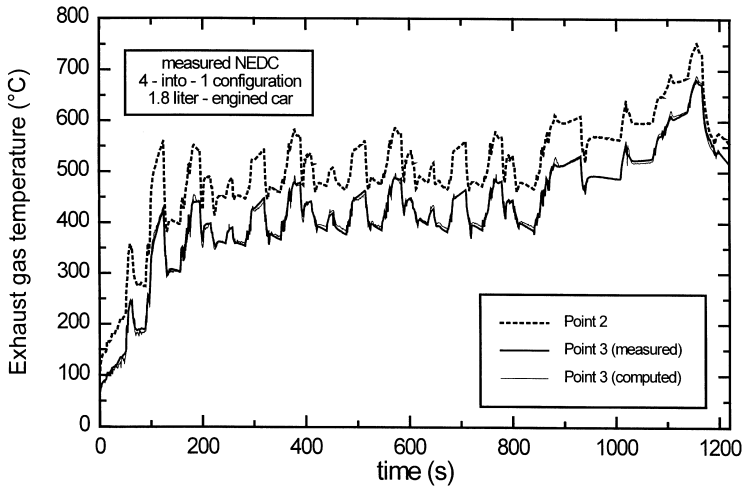

Fig. 5. Transient measurements results: four-into-one configuration. For comparison, the results of the computation are also shown.

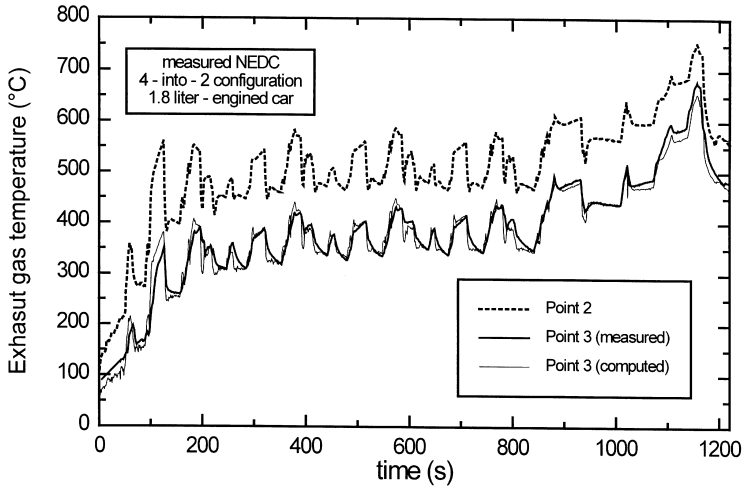

Fig. 6. Transient measurements results: four-into-two configuration. For comparison, the results of the computation are also shown.

four-into-one and the four-into-two exhaust system configurations. This is a good demonstration of the model validity and accuracy levels.

Next, we may proceed with a computation of another exhaust system configuration that is employed in a class of sports cars, namely, the four-into-catalyst configuration. In this case, there is no downpipe, and a stainless steel manifold with very long runners is ending very close to the converter inlet. Fig. 7 shows the results of a transient heat transfer computation with a four-into-catalyst configuration. For comparison reasons, exhaust temperatures at the reference point are taken equal to the curve of the corresponding point at the other configurations (see Fig. 1a–c).

According to the unified presentation of the computed temperatures at point 2 with the three

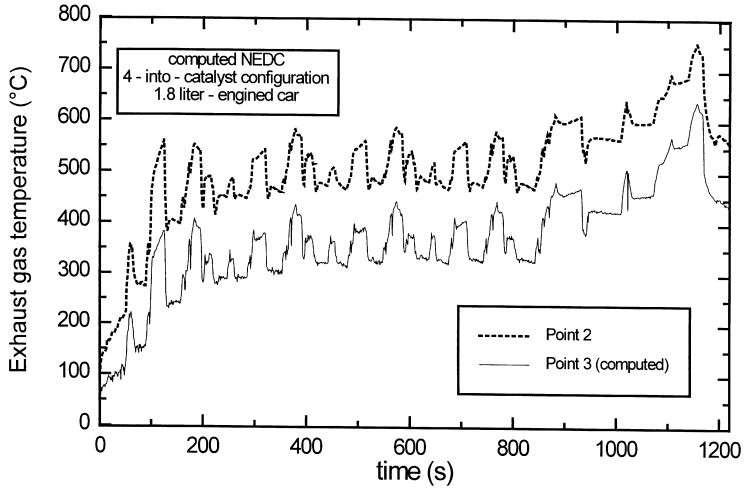

Fig. 7. Transient computation: four-into-catalyst configuration.

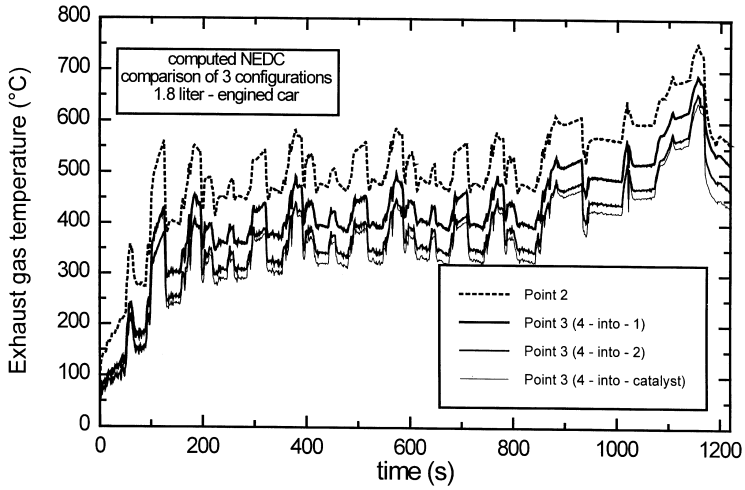

Fig. 8. Transient computation: Comparison of four-into-one, four-into-two and four-into-catalyst configurations.

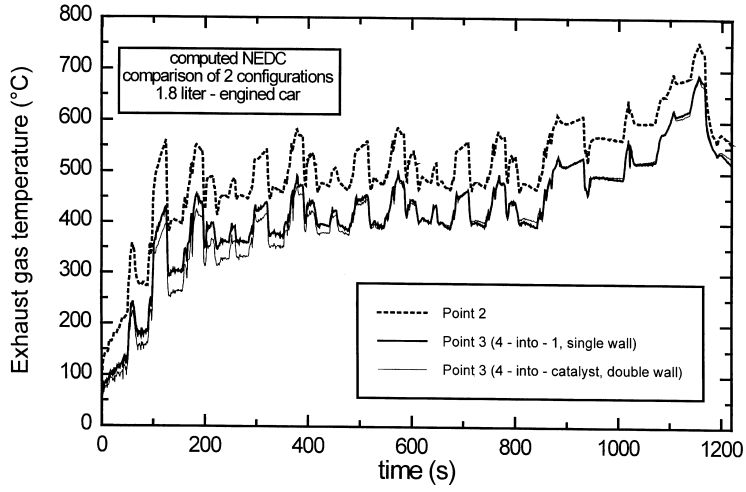

Fig. 9. Improvements by double-walled design: four-into-catalyst, double wall vs four into one single wall.

alternative configurations (Fig. 8), the configuration of Fig. 1(c) would be unfavorable for the catalytic converter light-off and global efficiency in view of the lower temperature levels.

A possible improvement to this situation could be effected by the shift to double-walled design. The results of this design modification are shown in Fig. 9, where a four-into-catalyst double walled downpipe configuration is compared to the standard four into one single walled design of Fig. 1(a).

5. Concluding remarks

When one faces the problem of defining an engineering approach to the design of a spark-ignition-engined vehicle exhaust system, that aims at the attainment of specific exhaust

emissions targets, high accuracy in heat transfer computations is imperative. Furthermore, the compromises related to converter efficiency and durability targets (catalyst aging) involve extensive heat transfer computations. Thus, an in depth study of exhaust piping heat transfer and the development of related exhaust system heat transfer codes are essential in supporting Computer Aided Engineering methodologies for exhaust after-treatment systems [5].

The following exhaust system design parameters may be optimized:

- exhaust manifold material, thickness and insulation
- exhaust manifold and downpipe design (geometry)
- position of catalytic converter in gasoline engines
- position of particulate trap in Diesel engines
- effect of distributed or concentrated metallic masses (e.g., flanges) on transient response
- different types of pipe insulation

Heat transfer models also support the design optimization of Diesel particulate trap systems [4], where the temperature levels are critical for particulate burn-off (regeneration). Other areas profiting from the detailed study of engine exhaust piping heat transfer are the design of fast response manifolds for turbocharged engined vehicles as well as acoustic modeling of exhaust systems.

In this paper, transient heat transfer in automotive exhaust systems was examined and a computer-aided approach to exhaust system temperature response optimization was employed in the study of real world design situations. A discussion of the work done so far in the determination of heat transfer rates, shows that knowledge in this area is yet rather inadequate for the purposes of transient computations in real exhaust systems. Thus, the authors employed a set of steady state tests on two different cars, along with transient tests during NEDC driving of a third car on the chassis dyno, with alternative exhaust and downpipe designs, in order to better understand the situation. The procedure resulted in a more complete understanding of the Nu–Re relationship in both steady state and transient engine operation. The results of the computational model compared particularly well with the transient exhaust temperature measurements on the chassis dyno.

The exhaust system heat transfer model presented in this paper, in cooperation with complementary codes, which simulate the transient behavior of exhaust after-treatment devices (e.g., catalytic converters or particulate traps), may support a complete and efficient methodology for exhaust systems design optimization.

Acknowledgements

The authors wish to thank Dr G.C. Koltsakis and Dr P.A. Konstantinidis, who wrote the LAT exhaust system heat transfer codes employed in the computational runs of this paper. Also, they wish to thank Mr Luciano Mina and Giovanni Guenna of the CRF for the many useful feedbacks and discussions, as well as measurement data communicated during the last five years.

References

[1] Huber EW, Koller T. Pipe Friction and Heat Transfer in the Exhaust Pipe of a Firing Combustion Engine. Tokyo: CIMAC Congress, 1977.
[2] Quarg J. Zur Berechnung des Wärmeüberganges in Abgaskrümern. MTZ 48, 7/8, 1987.
[3] Konstantinidis PA, Koltsakis GC, Stamatelos AM. Transient heat transfer modeling in automotive exhaust systems. In: Proc Inst Mech Engrs, Part C: J Mech Eng Sci 1997;211:1–15.
[4] Pattas KN, Stamatelos AM, Constantinidis J. Exhaust temperature response of trap oxidizer systems, 1990 SAE paper 900323.
[5] Konstantinidis PA, Koltsakis GC, Stamatelos AM. The role of CAE in the design optimization of exhaust aftertreatment systems. In: Proc Inst Mech Engrs, Part D: Journal of Automobile Engineering 1998;212:169–86.
[6] Caton JA, Heywood JB. An experimental and analytical study of heat transfer in an engine exhaust port. Int J Heat Mass Transfer 1981;24(4):581–95.
[7] Frank RM. A computer model for the heat loss in the exhaust manifold of an internal combustion engine. S.M. Thesis, Department of Mechanical Engineering, Massachusetts Institute of Technology, May 1986.
[8] Meisner S, Sorenson SC. Computer simulation of intake and exhaust manifold flow and heat transfer, 1986 SAE paper 860242.
[9] Sachdev R. An investigation of instantaneous heat transfer rates in the exhaust port of an internal combustion engine. M.S. thesis, Department of Mechanical and Industrial Engineering, University of Illinois, Urbana, Illinois 1981.
[10] Zhang Y, Phaneuf K, Hanson R, Showalter N. Computer modeling on exhaust system heat transfer, 1992 SAE paper 920262.
[11] Chen DKS. A numerical model for thermal problems in exhaust systems, 1993 SAE paper 931070.
[12] Liu Z, Hoffmanner AL, Skowron JF, Miller MJ. Exhaust transient temperature response, 1995 SAE paper 950617.
[13] Caton JA. Heat transfer, mixing and HC oxidation in an engine exhaust port. Ph.D. Thesis, MIT 1979.
[14] Caton JA. Comparisons of thermocouple, time-averaged, and mass-averaged exhaust gas temperatures for a spark-ignited engine, 1982 SAE 820050.
[15] Sieder EN, Tate E. Heat transfer and pressure drop of liquids in tubes. Ind Eng Chem 1936;28:1429.
[16] Gnielinski V. Int Chem Eng 1976;16:359.
[17] Kays WM, Crawford ME. Convective Heat and Mass Transfer, 2nd ed. New York: McGraw-Hill, 1980.
[18] Reynolds HC, Swearingen TB, McEligot DM. Journal of Basic Engineering 1969;91:87–94.
[19] Rohsenow WM, Hartnett JP, Ganic EN. Handbook of Heat Transfer Fundamentals, 2nd ed. New York: McGraw-Hill, 1985.
[20] Hausen H. Heat Transfer in Counter Flow, Parallel Flow and Cross Flow. New York: McGraw-Hill, 1983.
[21] Ede AJ. The effect of a right-angled bend on heat transfer in a pipe, International Developments in Heat Transfer 1961;634–642.
[22] Condie KG, McEligot DM. Convective Heat Transfer in Exhaust System Components for Start-up Emission Control, 1994 ISATA Conference.
[23] Sandford MH, Jones RD. Powerplant systems and the role of CAE—Part 1. Exhaust systems, 1992 SAE paper 920396.
[24] Benson RS. Numerical solution of one-dimensional non-steady flow with supersonic and subsonic flow and heat transfer. Journal of Mechanical Engineering Science 1972;14:635–42.
[25] Wendland DW. Automobile exhaust-system steady-state heat transfer, 1993 SAE paper 931085.
[26] Waermeatlas. Düsseldorf: VDI-Verlag, 1988.
[27] Hottel HC, Sarofing AF. Radiative Heat Transfer. New York: McGraw-Hill, 1967.
[28] Geidt WH. Principles of Engineering Heat Transfer. New York: Van Nostrand Company, 1957.
[29] Incropera FP, DeWitt DP. Fundamentals of Heat and Mass Transfer, 3rd ed. New York: Wiley, 1990.